

General Basis Functions for Parametric Representation of Energy Deposition Processes

S.G. Lambrakos

(Submitted December 19, 2008)

General basis functions for parametric representation of energy deposition processes are constructed according to the general physical characteristics of energy deposition within a volume of material from a beam energy source. These basis functions include previously constructed source functions as special cases. The construction of a general parameterization of energy deposition processes, e.g., welding and rapid prototyping, is necessary for inverse analysis of such processes. The structure of such a parameterization follows from the concepts of model and data spaces that imply the existence of an optimal parametric representation for a given class of inverse problems. Accordingly, the optimal parametric representation lying within the model space is determined by the characteristics of the available data, i.e., data space, which contain both experimental measurements and numerical simulation data. Experimental measurements include solidification cross-sections, thermocouple measurements, and microstructural changes. Numerical simulation data include general temperature field trend characteristics, response characteristics of materials to volumetric energy deposition, and the relative sensitivity of temperature field characteristics to phenomena occurring on different space and time scales. A general procedure is described for using basis functions with the available experimental and numerical data to construct a multidimensional field representation of a large class of energy deposition processes.

Keywords joining, modeling processes, welding

1. Introduction

The inverse problem approach is optimal for system characterization in that it tends to adopt large amounts of available data for model input (Ref 1-9). Accordingly, large amounts of information obtained from both experimental measurements and numerical simulations are not wasted. This follows from the fact that input and output quantities tend to be significantly different in the case of inverse analysis in contrast to that of direct analysis that is based on first principles. There exist many fine surveys on inverse analysis. These surveys and their associated critiques are with respect to various types of systems, inverse methods of analysis, and associated paradigms for application of these methods. Considered here is a particular class of inverse analysis methods that are applied to energy deposition processes where the available data consist of temperature distributions over and within bounded spatial domains. Or equivalently, the available data consist of temperatures distributed over essentially closed surfaces spanning regions of finite volume containing materials of interest. In what follows, general concepts are presented for inverse analysis that are based on specific paradigms and various mathematical properties that follow from these paradigms. In particular, the general framework of

inverse methods applied to data sets containing measurements over a bounded finite volume system can be cast into the formalism of geometric inverse problems (Ref 8) whose general form is that of an elliptic boundary value problem defined over an essentially closed domain with Dirichlet or Neuman boundary conditions. With respect to energy deposition processes this implies that in practice no matter what the form of the “solver” employed, where different solvers correspond to different assumptions of the field equations representing the system, the influence of constraints derived from the general characteristics of the available data is such that those terms not related to solution of an elliptic boundary value problem are essentially extraneous. This property follows from the nature of data driven inversion. This property is relatively subtle in that it is difficult to prove in general, “on the one hand”, and yet reasonably obvious on the other. Accordingly, any field quantity that is specified over a closed domain will have imposed on its structure relatively stringent geometric properties associated with elliptic boundary value problems. That is to say, even if the physical nature and associated basic theory underlying an energy deposition process implies a specific set of representative field equations and boundary conditions, which do not correspond to an elliptic boundary value problem, the structure of the data space for inverse analysis of this system is such that the formal structure of an elliptic boundary value problem is imposed.

Inverse analysis within the context of system identification theory is according to two different approaches. One of these approaches is that of a “gray box” parametric representation where the mathematical model adopted, although consisting of adjustable parameters, has a mathematical structure that is consistent with the physical nature of the system. The other approach is that of a “black box” parametric representation

S.G. Lambrakos, Center for Computational Materials, Code 6390, Materials Science and Technology Division, Naval Research Laboratory, Washington, DC. Contact e-mail: lambrakos@anvil.nrl.navy.mil.

where the model adopted consists of adjustable parameters associated with a mathematical structure that is an optimal mapping from data to system output without any consideration of the underlying physical nature of the system. The direct-problem approach, where the mathematical representation of the system is based entirely on first principles, implies a “white box” representation.

Direct and inverse problem formulations possess an important interrelationship, which is that parametric model representations derived from basic physical theory can be adopted for inverse analysis. This interrelationship implies that a reasonable starting point for the formulation of an inverse problem based parametric representation is to adopt a direct-problem based parametric representation as an initial ansatz for further modification (or optimization) according to the characteristics of the experimental or numerical simulation data concerning the field quantities of interest. It is with respect to this interrelationship that one defines the “gray box” approach for system identification. Our emphasis in this work is inverse analysis whose formal structure is that of a “gray box.”

Certain perceptions have been associated with inverse analysis due to its interrelationship with direct analysis. Among these are that computational costs and errors associated with inverse analyses are comparable to those of direct analyses. The computational cost of inverse analyses, however, should be, in general, less than that of analyses based on the direct-problem approach since one considers for inverse analysis not only parameter optimization but also model optimization relative to the available data. Similarly, it should not be expected that computational errors associated with inverse analysis are comparable to those of direct-problem analyses since one can in principle apply in inverse analysis an optimal map from data space to model space in terms of the formal mathematical representation as well as the discrete numerical algorithm and computational platform. In inverse analysis it is not the nature of the system that primarily determines the model representation, but rather the nature of the experimental measurements and numerical simulations that are available for construction of the system data space.

The determination of the temperature field within a bounded domain defines the inverse heat deposition problem, which represents a particular category of the more general inverse problem concerning inverse analysis of heat transfer (Ref 10-18). Other investigators have also focused on various aspects of inverse problems related to heat deposition processes especially as they relate to the determination of heat fluxes via appropriate regularization of their spatial and time distributions (Ref 19). General aspects of the inverse problem approach presented here, for the analysis of heat deposition processes, have been studied (Ref 20-30). These studies considered the specific physical characteristics of heat deposition processes that are relevant to using this inverse problem approach for their analysis. This approach included the use of effective material properties and heat source distributions as adjustable quantities. These quantities are adjusted according to experimental data in order to constrain the temperature field self-consistently. Throughout these studies prototype analyses were presented in order to demonstrate many of the details associated with practical application of this inverse problem approach and its use for extraction of process parameters and parameters that may be correlated with material properties. The general parameterization of heat

deposition systems follows from the concept of a model space that establishes the existence of an optimal parametric representation for a given class of inverse problems. This property is related to the fact that inverse analyses based entirely on mathematical formulations representing physical theories are not generally well posed in that these formulations are inherently based on direct-problem paradigms. The term “well posed” here for an inverse problem is used in the sense of Hadamard (Ref 31), which is such that a problem is well posed if a solution exists, this solution is unique and it depends continuously on the data. In particular, the concept of a model space implies the existence of an optimal parametric representation for inverse analysis, which is not based on the existence of a complete set of representative physical theories, but rather on the characteristics, relative sizes, and completeness of data sets associated with or in practice available for that system.

Owing to the enormity of analyses associated with energy deposition processes, it is extremely difficult to denumerate as well as critique all the relevant work. The enormity of these analyses, however, has resulted in a situation where there already exist many comprehensive reviews, although of differing perspectives, concerning the construction of parametric model representations of energy deposition processes. Among the collected works, within which there have been many comprehensive reviews concerning energy deposition processes, are the “Trends in Welding” series (Ref 32), the Mathematical Modelling of Weld Phenomena” series (Ref 33), and the works of Goldak et al. (Ref 34-36). An interesting aspect of these collected works is that in many of the studies included therein the methodology employed for analysis is that of inverse analysis without explicit reference to this fact, while in other studies methodologies for inverse analysis are presented that retain certain features based on direct-problem paradigms. This situation follows naturally from the fundamental interrelationship of direct and inverse problem formulations.

In previous studies concerning inverse analysis using the approach considered here, a relatively exhaustive collection of prototype analyses were presented. Accordingly, this study does not describe new prototype analyses for the purpose of demonstrating applications of inverse analysis to different types of energy deposition processes. In addition, for purposes of the present study, it is not necessary to present any new experimental measurements concerning energy deposition processes. The goal of the present study is to describe a general procedure for using basis functions with the available experimental and numerical data to construct a multidimensional field representation of a large class of energy deposition processes. Therefore, it is significant to note that the available experimental and numerical data resulting from previous studies (again, too many to denumerate) are sufficient for this goal.

The organization of the subject areas presented here are as follows. First, general concepts that establish the foundation of the specific inverse analysis approach considered here are discussed. These include the concepts of data and model space, generalized functions, parametric representations using basis functions, numerical simulation data, general characteristics of energy deposition processes, and the volumetric energy source function. Second, a precise mathematical statement of the inverse problem to which the analysis methodology is to be applied is given. In that the range of inverse problems is vast, it

is essential, even within the context of inverse heat transfer, to define precisely the inverse problem to be addressed. Third, general basis functions are constructed for the separate spatial domains characterizing energy deposition processes. Fourth, inverse analysis is applied to Gas Metal Ark weld of steel for the purpose of providing an illustrative example of some specific aspects of energy deposition processes. Finally, a general procedure is described for construction of a multidimensional field representation of a large class of energy deposition processes.

2. Concepts Adopted for Construction of Basis Functions

2.1 Model Space and Data Space

Following the inverse problem approach, a system is represented by a model and associated set of adjustable parameters. The particular choice of a model (or equivalently, model and associated set of parameters) is termed a “parameterization” of the system. The choice of a particular parameterization to be used to describe a system, however, is in general not unique. In order to address the property of non-uniqueness of system parameterization, inverse problem theory has adopted the concepts of “model space,” where each point of this space represents a “conceivable” model of the system, and “data space,” where each point of this space represents available data sets or potentially feasible measurements and characteristics of data sampling for purposes of parameter determination via appropriate optimization methods (Ref 3). Accordingly, an optimal parametric representation within the model space is determined by the characteristics of the associated data space. Given a model space of a specific system, quantitative inverse analysis of the system is further enhanced by isolating the regions of model space that correspond to parameterizations that are both physically consistent and sufficiently general in terms of their mathematical representation. The inverse-analysis methodology that is presented in this study adopts parameterizations that are in terms of weighted sums of basis functions.

2.2 Generalized Functions

A generalized function is defined as a function representation of a class of functions, rather than a specific function, where the class of functions is characterized by a specific set of trend features (Ref 37). This concept was introduced in signal processing, where for many analysis applications-specific trend features are of significance rather than specific analytical forms. For example, functions such as the unit step function, rectangle function, and delta function are not represented by specific analytical forms but by sets of functions having the same general trend features. In what follows, the concept of generalized functions is extended for the construction of general basis functions for parametric representation of energy deposition processes.

2.3 Parametric Function Representation Based on Basis Functions

The inverse analysis approach considered here considers a less general model space where each point of this space

represents a set of basis functions, in contrast to any “conceivable” model, for parametric representation in terms of weighted sums of these functions. The specific set of basis functions are to be selected according to two criteria. These are their relative optimality for establishing a mapping from data space to system output and for the inclusion of information concerning physical characteristics of the system, i.e., a gray box parametric representation.

2.4 General Characteristics of Energy Deposition

The inverse analysis approach considered here assumes a general partitioning of energy deposition processes into three separate and phenomenologically coupled spatial domains (see Fig. 1). One domain is that above the surface of the workpiece, which contains the beam source and its interaction with the workpiece surface. Another domain is that containing the volumetric distribution of energy within the material of the workpiece. And another domain is that containing the temperature field distribution within the workpiece. The nature of the coupling between these three domains is assumed phenomenological in that the characteristic time and spatial scales for the physical processes in each of these domains are significantly different from those of the others. An advantage of the inverse analysis approach is that an explicit consideration of the nature of the coupling between these domains is not necessary. An important aspect of the temperature field distribution associated with energy deposition processes is the presence of two types of weighting (see Fig. 2). These are weighting due to the presence of a surface boundary that is at the origin of coupling of energy into the system, and weighting due to the relative motion of the energy source and workpiece. The presence of these weightings provides for filter properties that tend to make the temperature field distribution insensitive to small-scale temporal and spatial features of the volumetric distribution of energy.

2.5 Numerical Simulation Data

The inverse analysis approach considered here adopts the perspective of computational physics, according to which a numerical simulation represents another source of “experimental” data. This perspective is significant in that a general procedure may be developed that uses basis functions with both experimental and numerical data to construct a

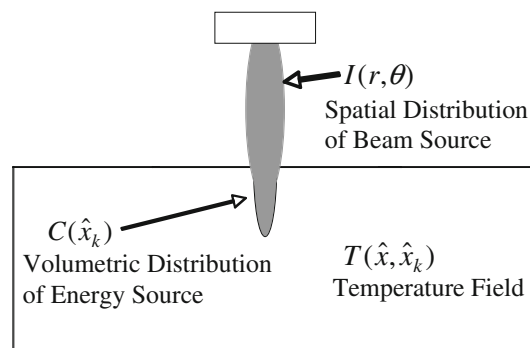


Fig. 1 Schematic representation of three domains characterizing energy deposition processes, beam-surface interaction, volumetric energy deposition, and temperature field distribution

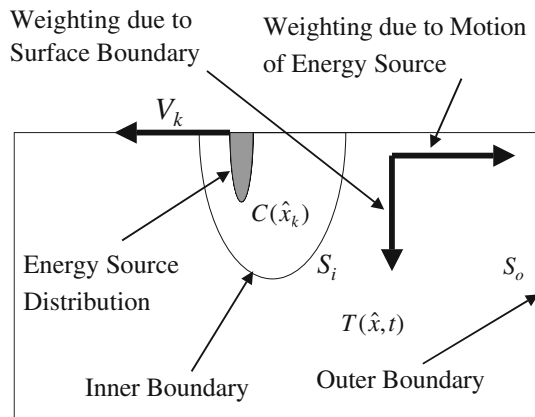


Fig. 2 Schematic representation of inner and outer boundaries of temperature field that define inverse heat deposition problem, and weighting influences on temperature field associated with energy deposition

multidimensional field representation of a large class of energy deposition processes.

2.6 Volumetric Energy Source Function

The volumetric energy source function, or equivalently, parametric representation of the volumetric distribution of energy within the material of the workpiece, is the primary component for mathematical representation of energy deposition processes for both direct and inverse analyses. Accordingly, many researchers have constructed different types of source functions for different types of energy deposition processes (Ref 34-58). A review of the different source function formulations from the perspective of inverse analysis, however, shows that these functions are within a specific class of functions. Therefore, it follows that one can construct a “generalized function” representation of the volumetric distribution of energy that includes previously constructed source functions as special cases.

3. Definition of Inverse Heat Deposition Problem

The inverse problem concerning analysis of physical processes, in general (Ref 1-9), and the inverse heat transfer problem, in particular (Ref 10-18), may be stated formally in terms of source functions (or input quantities) and multidimensional fields (output quantities). The statement of the inverse problem given here is focused on aspects of the inverse heat deposition problem related to the determination of heat fluxes via appropriate regularization of their spatial and time distributions. This statement represents an extension of that given in Ref 19. In general, the formulation of a heat conductive system occupying an open bounded domain Ω with an outer boundary S_o and an inner boundary S_i involves the parabolic equation

$$\frac{\partial T(\hat{x}, t)}{\partial t} = \nabla \cdot (\kappa(\hat{x}, t) \nabla T(\hat{x}, t)) \quad (\text{Eq 1a})$$

for $T(\hat{x}, t)$ in $\Omega \times (0, t_f)$, with initial condition $T(\hat{x}, 0) = T_0(\hat{x})$ in Ω , and heat flux exchanges through the outer and inner boundaries S_o and S_i as follows:

$$-\kappa(\hat{x}, t) \frac{\partial T(\hat{x}, t)}{\partial n_{S_o}} = c(\hat{x}, t)(T(\hat{x}, t) - T_a(\hat{x}, t)) \quad (\text{Eq 1b})$$

on $S_o \times (0, t_f)$, and

$$-\kappa(\hat{x}, t) \frac{\partial T(\hat{x}, t)}{\partial n_{S_i}} = q(\hat{x}, t) \quad (\text{Eq 1c})$$

on $S_o \times (0, t_f)$. Here $\hat{x} = (x, y, z)$ is the position vector, n_{S_o} and n_{S_i} are the normal vectors onto boundary S_o and S_i , respectively, t is the time variable, t_f is the final time, $T(\hat{x}, t)$ is the temperature field variable, $\kappa(\hat{x}, t)$ is the thermal diffusivity field variable, $c(\hat{x}, t)$ and $T_a(\hat{x}, t)$ are specified functions, and $q(\hat{x}, t)$ is the heat flux on the inner boundary S_i . Determination of the temperature field via solution of Eq 1a-c defines the direct initial-boundary value problem. The inverse problem considered here is that of effectively reconstructing the heat flux field $q(\hat{x}, t)$ on the inner and outer boundaries S_i , and the resulting temperature field $T(\hat{x}, t)$ for all time $t \in [0, t_f]$ when S_i and S_o are totally or partially inaccessible. In order to reconstruct the heat flux, information on the temperatures $T(\hat{x}_S, t)$, where $\{\hat{x}_S\} \in S_i, S_o$ is needed and therefore must be acquired either experimentally or via direct numerical simulation (Ref 20-30).

Following the gray box inverse analysis approach, a parametric representation based on a physical model provides a means for the inclusion of information concerning the physical characteristics of a given energy deposition process. It follows then that for heat deposition processes involving the deposition of heat within a bounded region of finite volume, consistent parametric representations of the temperature field are given by

$$T(\hat{x}, \kappa, t) = T_A + \sum_{k=1}^{N_k} T_k(\hat{x}, \hat{x}_k, \kappa, t; \alpha_1, \dots, \alpha_n) \quad (\text{Eq 2})$$

and $T(\hat{x}_n^c, t_n^c, \kappa) = T_n^c$

where the quantity T_A is the ambient temperature of the workpiece and the locations \hat{x}_n^c and temperature values T_n^c specify constraint conditions on the temperature field. The functions $T_k(\hat{x}, \hat{x}_k, \kappa, t; \alpha_1, \dots, \alpha_n)$ represent an optimal basis set of functions for given sets of boundary conditions and material properties. The quantities $\hat{x}_k = (x_k, y_k, z_k)$, $k = 1, \dots, N_k$, are the locations of the elemental source or boundary elements. The sum defined by Eq 2 can for certain systems specify numerical integration over the discrete elements of a distribution of sources or boundary elements. Selection of an optimal set of basis functions is based on a consideration of the characteristic model and data spaces of heat deposition processes and subsequently isolating those regions of the model space corresponding to parameterizations that are both physically consistent and sufficiently general in terms of their mathematical representation and mapping from data to model space. Although heat deposition processes may be characterized by complex coupling between the heat source and workpiece, as well as complex geometries associated with either the workpiece or deposition process, in terms of inverse analysis the general functional forms of the temperature fields associated with all such processes are within a restricted class of functions, i.e., optimal sets of functions. Accordingly, a sufficiently optimal set of functions are the analytic solutions to heat conduction equation for a finite set of boundary conditions (Ref 59). A parameterization based on this set is both sufficiently general and convenient relative to optimization.

The formal procedure underlying the inverse method considered here entails the adjustment of the temperature field defined over the entire spatial region of the sample volume at a given time t . This approach defines an optimization procedure where the temperature field spanning the spatial region of the sample volume is adopted as the quantity to be optimized. The constraint conditions are imposed on the temperature field spanning the bounded spatial domain of the workpiece by minimization of the value of the objective functions defined by

$$Z_T = \sum_{n=1}^N w_n (T(\hat{x}_n^c, t_n^c, \kappa) - T_n^c)^2 \quad (\text{Eq 3})$$

where T_n^c is the target temperature for position $\hat{x}_n^c = (x_n^c, y_n^c, z_n^c)$.

The input of information into the inverse model defined by Eq 1 to 3, i.e., the mapping from data to model space, is effected by the assignment of individual constraint values to the quantities T_n^c ; the form of the basis functions adopted for parametric representation; and specifying the shapes of the inner and outer boundaries, S_i and S_0 , respectively, which bound the temperature field within a specified region of the workpiece. The constraint conditions and basis functions, i.e., $T(\hat{x}_n^c, t_n^c, \kappa) = T_n^c$ and $T_k(\hat{x}, \hat{x}_k, \kappa, t; \alpha_1, \dots, \alpha_n)$, respectively, provide for the inclusion of the following types of information: (a) solidification cross-sections (e.g., transverse, longitudinal, and top surface cross-sections); (b) spatial character of energy source (e.g., position of maximum temperature, shape and relative location of keyhole in deep-penetration welds); (c) geometric information (e.g., shape features of workpiece and top surface of weld); (d) boundary conditions on workpiece; (e) information related to temperature history (e.g., microstructure correlation with temperature); (f) thermocouple measurements; (g) energy input (e.g., energy per distance); and (h) information based on physical model representations of aspects of heat deposition process.

In a previous study (Ref 20), a partial proof was constructed for the existence of a general parametric representation for inverse analysis of heat deposition processes. This proof was considered partial in the sense that certain aspects of its development should be made more precise and investigated in more detail with respect to practical application. The essential components of this proof are as follows. First, the general trend features of heat deposition processes are such that the construction of a complete basis set of functions $T_k(\hat{x}, \hat{x}_k, \kappa, t; \alpha_1, \dots, \alpha_n)$ making up a linear combination of the form defined by Eq 2 for representation of the associated temperature field is well defined and readily achievable. Second, for heat deposition processes, characteristics of the temperature field are poorly correlated to characteristics of the energy source. The characteristics of the temperature field that are associated with these processes, however, are strongly coupled only to inner boundaries on this field, e.g., the solidification boundary. This property follows from the low-pass spatial filtering property of the basis functions $T_k(\hat{x}, \hat{x}_k, \kappa, t; \alpha_1, \dots, \alpha_n)$, whose general forms are consistent with the dominant trend features of heat deposition processes. Third, given a consistent set of basis functions, the temperature field associated with a heat deposition process is completely specified by the shape and temperature distribution of a given inner boundary on the domain of the temperature field, the diffusivity κ and

speed of deposition V , and the lengths of the spatial dimensions D_i of the workpiece. Fourth, the shape and temperature distribution of a specified inner boundary S_i is determined by the rate of energy deposited on the surface of the workpiece Q_{HDP} and the strength of coupling of the energy source to the workpiece γ . As demonstrated via constructive proof (Ref 20), for any given inner boundary, e.g., solidification boundary, there exists a multidimensional temperature field $T(\hat{x}, \kappa, V, D_i)$, where $i = 1$ and $i = 1, 2$ for structures of finite thickness and cross section, respectively, such that

$$\gamma Q_{\text{HDP}}(I(r, \theta)) = Q_{\text{WCH}}(T(\hat{x}, \kappa, V, D_i)) \quad (\text{Eq 4})$$

where $\hat{x} = (x, y, z)$ and Q_{WCH} is the energy that has been coupled into the workpiece and is given by

$$Q_{\text{WCH}} = \int_{x_1}^{x_2} \int_{y_1}^{y_2} \int_{z_1}^{z_2} \left[\int_{T_A}^{T(x,y,z)} \rho(T) C_p(T) dT \right] dx dy dz \quad (\text{Eq 5})$$

for energy deposition within a sample volume $V_S = (x_2 - x_1)(y_2 - y_1)(z_2 - z_1)$. As indicated in Eq 4, Q_{HDP} is a function of the spatial distribution $I(r, \theta)$ of the beam above the workpiece. Referring to Eq 4, it is to be noted that although the quantity γ is dependent upon the nature of the heat deposition process, a general characterization of Q_{WCH} is well posed based on the geometric structure of energy deposition profiles only. And finally, in that an inner boundary S_i (see Fig. 1) is defined by its shape and the distribution of temperatures on its surface $T(\hat{x}_S)$, it follows that one can define a multidimensional temperature field $T(\hat{x}, \kappa, V, D_i, T(\hat{x}_S), \hat{x}_S \in S_i)$.

The existence of a convenient and general parameterization of inner boundary surfaces, $T(\hat{x}_S), \hat{x}_S \in S_i$, bounding the temperature fields associated with heat deposition processes is conjectured based on the obvious fact that all heat deposition processes are characterized by thermal and energy deposition profiles whose general form can be represented by a small class of geometric shapes. This conjecture is plausible and is based on the fact that the observed volumetric distributions of energy from all types of heat deposition processes, within the inner boundary S_i of their associated temperature fields, can be represented by linear combinations of the basis functions that are extensions of the Beer-Lambert law. In the sections that follow, a modified Beer-Lambert expression is constructed based on physical arguments that provide for extension of the Beer-Lambert law. These arguments, which represent the essential components of a constructive proof, establish a plausible foundation for the existence of a relatively optimal and general parametric representation $T(\hat{x}, \kappa, V, D_i, T_b(\hat{x}_S), \hat{x}_S \in S_i, S_0)$ for inverse analysis of heat deposition processes. In doing so, referring to Fig. 2, the inverse problem defined by the mapping

$$C(\hat{x}_k) \mapsto T(\hat{x}) \quad (\text{Eq 6})$$

is replaced by the inverse problem defined by the mapping

$$C(\hat{x}_k), \kappa \mapsto S_i, S_0 \mapsto T(\hat{x}). \quad (\text{Eq 7})$$

Following the same arguments, the definition of the inverse heat deposition problem as given above can be extended to include systems that are characterized by incomplete information concerning the diffusivity function κ . This would include

any nonlinear dependence of κ on temperature. This follows in that Eq 7 implies the existence of a weighted space averaged diffusivity.

Given an inverse analysis formulation that is defined by the sequence of mappings Eq 7, relatively interesting sensitivity issues are observed to follow. The mathematical properties underlying these sensitivity issues are the same as those responsible for the ill posedness of many inverse analysis procedures based on the mapping Eq 6. That is to say, those filter properties of diffusion processes that tend to make the temperature field $T(\hat{x})$ insensitive to details of the shape of the source distribution $C(\hat{x}_k)$, tend to make $T(\hat{x})$ insensitive to details of the shapes of S_i and S_0 . This insensitivity to details of the shapes of S_i and S_0 , e.g., the shape of the solidification boundary, implies that a general parametric representation of the inner and outer boundaries can in principle be formulated in terms of a reasonably convenient mathematical form. Presented in next sections are sensitivity analyses examining the sensitivity of $T(\hat{x})$ to shape features of S_i and S_0 and relevance for inverse heat deposition analysis based on the sequence of mappings Eq 7. For these analyses the heat source distribution assumes the role of a boundary surface generator. This interpretation of $C(\hat{x}_k)$, which permits its convenient parameterization, provides a framework for parametrization of S_i and S_0 .

In that energy deposition processes can in general be characterized by three separate spatial domains corresponding to a beam energy source, volumetric energy deposition, and temperature field distribution, where the degree and nature of the coupling between these domains is a characteristic of the specific process, it follows that a consistent representation of the temperature field in terms of basis functions is of the form

$$T(\hat{x}, t) = T_A + \sum_{k=1}^{N_k} \sum_{n=1}^{N_t} C_k(\hat{x}_k, n\Delta t) F_k(\hat{x}, \hat{x}_k, n\Delta t, \kappa, V_k), \quad (\text{Eq 8})$$

where

$$C_k(x, y, z_0) = \gamma_k I(r, \theta), \quad (\text{Eq 9})$$

$t = N_t \Delta t$, $r = (x^2 + y^2 + z_0^2)^{1/2}$ and $\sin \theta = z_0/r$, where z_0 is relative to the origin of the beam energy source whose spatial distribution is $I(r, \theta)$. In the case of steady state deposition, the parameters Δt and N_t are assigned values such that time t is sufficiently long. The strength of coupling of the energy source to the workpiece γ_k , essentially the same quantity defined in Eq 4, is dependent upon the nature of the heat deposition process. The general procedure for calculation of temperature fields for energy deposition processes using the inverse analysis approach considered here is shown in Fig. 3.

4. Basis Functions for Representation of Field Function $F_k(\hat{x}, \hat{x}_k, n\Delta t, \kappa, V_k)$

A general temperature field parameterization for energy deposition processes is constructed based on general physical characteristics of energy deposition within a volume of material. This parameterization, or set of basis functions, includes previously constructed parameterizations as special cases. Proceeding, it follows that for a constant diffusivity κ , Eq 1a assumes the form

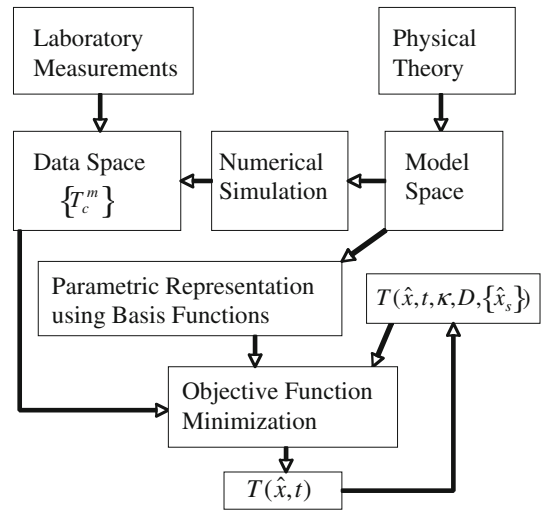


Fig. 3 General procedure for calculation of temperature fields for energy deposition processes using inverse analysis

$$\frac{\partial T(\hat{x}, t)}{\partial t} = \kappa \nabla^2 T(\hat{x}, t). \quad (\text{Eq 10})$$

Next, solving Eq 10 for the boundary condition $T(\hat{x}, 0) = \delta(\hat{x})$, where $\delta(\hat{x})$ is the Dirac delta function, it follows that

$$T(\hat{x}, t) = \frac{1}{(4\pi\kappa t)^{d/2}} \exp\left[-\frac{x^2 + y^2 + z^2}{4\kappa t}\right] \quad (\text{Eq 11})$$

where the parameter d has a value according to the dimensionality of the heat diffusion. This follows from the global normalization condition

$$\int_{-\infty}^{\infty} \int_{-\infty}^{\infty} \int_{-\infty}^{\infty} T(\hat{x}, t) dx dy dz = 1 \quad (\text{Eq 12})$$

for three-dimensional heat diffusion. Accordingly, a relatively general set of basis functions for representation of the temperature field is given by

$$F_k(\hat{x}, \hat{x}_k, n\Delta t, \kappa, V_k) = \frac{1}{(n\Delta t)^{3/2}} \exp\left[-\frac{[x - x_k - V_k(n\Delta t)]^2 + (y - y_k)^2 + (z - z_k)^2}{4\kappa(n\Delta t)}\right] \quad (\text{Eq 13})$$

for heat diffusion whose general trend is characteristically three dimensional,

$$F_k(\hat{x}, \hat{x}_k, n\Delta t, \kappa, V_k) = \frac{1}{(n\Delta t)} \exp\left[-\frac{[x - x_k - V_k(n\Delta t)]^2 + (y - y_k)^2}{4\kappa(n\Delta t)}\right] \times \left\{ 1 + 2 \sum_{m=1}^{\infty} \exp\left[-\frac{\kappa m^2 \pi^2 (n\Delta t)}{l^2}\right] \cos\left[\frac{m\pi z}{l}\right] \cos\left[\frac{m\pi z_k}{l}\right] \right\} \quad (\text{Eq 14})$$

for heat diffusion whose general trend is characteristically two dimensional, and

$$\begin{aligned}
F_k(\hat{x}, \hat{x}_k, n\Delta t, \kappa, V_k) &= \frac{1}{\sqrt{(n\Delta t)}} \exp\left[-\frac{[x - x_k - V_k(n\Delta t)]^2}{4\kappa(n\Delta t)}\right] \\
&\times \left\{ 1 + 2 \sum_{m=1}^{\infty} \exp\left[-\frac{\kappa m^2 \pi^2 (n\Delta t)}{a^2}\right] \cos\left[\frac{m\pi y}{a}\right] \cos\left[\frac{m\pi y_k}{a}\right] \right\} \\
&\times \left\{ 1 + 2 \sum_{m=1}^{\infty} \exp\left[-\frac{\kappa m^2 \pi^2 (n\Delta t)}{l^2}\right] \cos\left[\frac{m\pi z}{l}\right] \cos\left[\frac{m\pi z_k}{l}\right] \right\}
\end{aligned} \quad (\text{Eq 15})$$

for heat diffusion whose general trend is characteristically one dimensional. The functions $F_k(\hat{x}, \hat{x}_k, n\Delta t, \kappa, V_k)$ represent a relatively optimal basis set of functions for boundary conditions that are characteristic of energy deposition processes. These processes include energy deposition within plate structures of variable thickness and level of penetration (consistent with Eq 14) and structures having a finite cross section of variable size and relative dimensions (consistent with Eq 15). In the case of energy deposition processes where the coupling of energy into the workpiece is distributed over large surface areas, e.g., rapid prototyping, the energy source function is characterized by a dense surface distribution of elemental heat sources, thus imposing “apparent” nonconduction boundary conditions, Eq 13 can be adopted as a physically consistent representation.

5. Basis Functions for Representation of Volumetric Source Function

In that the mapping $C(\hat{x}_k) \mapsto S_i$ does not imply a unique energy source function $C(\hat{x}_k)$, the goal is to determine a relatively optimal basis function set for the generation of the inner surface boundary S_i . The construction of a general basis set for representation of $C(\hat{x}_k)$ is in terms of a series of physically based phenomenological extensions of the formalism of the Beer-Lambert law. A general volumetric source function parameterization is constructed based on the general physical characteristics of energy deposition within a volume of material. This source function has been extended to represent daughter or secondary processes associated with deposition and includes previously constructed source functions as special cases.

The energy deposition characteristics of transmission spectroscopies (electrons, photons, or energetic particles in general) or of plasma plume, electron, and laser beam processes can be represented to a first approximation by the Beer-Lambert law, which is given in naperian form for a one-dimensional system by

$$Q(z) = A \cdot \exp[-\mu_1 C \cdot z] \quad (\text{Eq 16})$$

where A is the initial energy or particle density (or incident intensity) at the origin o , Q is the density at a distance z from the origin, μ_1 is the extinction coefficient and C is the concentration of the ambient medium. Before proceeding, it is significant to note that Eq 16 represents a first order process. This representation can be extended to include higher order processes by assuming that these processes may be decomposed into a set of coupled first-order processes that may be characterized locally by Eq 16. This extension is effected via the Modified Beer-Lambert law

$$Q(z) = A \cdot \exp[-\mu_1 C \cdot z] + B(z) \cdot \exp[-\mu_2 C \cdot z] \quad (\text{Eq 17})$$

where

$$\begin{aligned}
B(z) &= c_1 A \int_0^{\infty} u_I(z') \cdot \exp[-\mu_1 C \cdot (z - z')] dz' \\
&= \left(\frac{c_1 A}{\mu_1 C} \right) (1 - \exp[-\mu_1 C \cdot z]),
\end{aligned} \quad (\text{Eq 18})$$

$$u_I(z) = \lim_{Z_0 \rightarrow 0} \left\{ 1 - \exp\left[-\frac{z}{Z_0}\right] \right\}, \quad (\text{Eq 19})$$

and c_1 is a proportionality constant. This relationship follows from the fact that physically the coefficient $B(z)$ is the integrated response of the ambient medium to the incident deposition process, e.g., electron beam. The step function $u_I(z)$ represents a unit step generation of daughter processes in neighborhood of $z = 0$. Changes in μ_1 , μ_2 and C as a function of z can be represented quasi-linearly by again assuming that Eq 17 represents a set of locally coupled first-order processes characterized locally by Eq 16. Accordingly,

$$\begin{aligned}
Q(z) &= A \cdot \exp[-\mu_1 C f_1(z) \cdot z - f_0] \\
&+ \left(\frac{c_1 A}{\mu_1 C} \right) \cdot (1 - \exp[-\mu_1 C f_3(z) \cdot z]) \exp[-\mu_2 C f_2(z) \cdot z]
\end{aligned} \quad (\text{Eq 20})$$

where

$$f_i(z) = \sum_{j=0}^2 C_{ij} z^j \quad (\text{Eq 21})$$

and the functions $f_i(z)$, $i = 1, 2, 3$, are path length factors, which account for increases in path length caused by scattering within the material, and f_0 is a geometry factor, which accounts for instrument geometry, e.g., shape or spatial profile of beam source, and represents a modification of the initial value A . Finally, combining Eq 20 and 21,

$$\begin{aligned}
Q(z) &= Q_1 \cdot \exp[-\alpha_1 z - \alpha_2 z^2] \\
&+ Q_2 \cdot (1 - \exp[-\beta_1 z - \beta_2 z^2]) \exp[-\gamma_1 z - \gamma_2 z^2]
\end{aligned} \quad (\text{Eq 22})$$

Next, it is observed that in general energy deposition within a volume of material is highly localized. This can be imposed formally by means of a “cutoff distance” parameter z_c using the relation

$$Q_c(z) = \max[Q(z) - Q(z_c), 0]. \quad (\text{Eq 23})$$

Next, based on observation, a relatively general representation of the energy deposit with respect to the x and y coordinates is the Gaussian function. Thus

$$C(\hat{x}) = \exp[-(ax^2 + by^2)] \cdot Q_c(z). \quad (\text{Eq 24})$$

Finally, following Galdak et al. (Ref 34-36), Eq 24 can be extended to represent the influence of weighting due to motion of the energy source relative to the workpiece. Accordingly, for motion of the energy source along the x coordinate,

$$\begin{aligned}
C(\hat{x}) &= ([1 - u(x)] \cdot \exp[-a_1 x^2] + u(x) \cdot \exp[-a_2 x^2]) \\
&\times \exp[-by^2] \cdot Q_c(z),
\end{aligned}$$

where $u(x)$ is the unit step function. At this stage a consideration of the physical nature of processes represented by

Eq 25 establishes a foundation for the generalized function representation of volumetric energy distribution associated with energy deposition processes. Referring to Eq 22, it is significant to note that its parameterization, although phenomenological, is based on general physical characteristics of energy deposition with respect to depth of penetration. These physical characteristics, however, are more generally represented by the generalized function Q_g shown in Fig. 4, which is defined by three dominant trend features that are associated with primary and secondary processes, and their extinction. By adopting the generalized function Q_g more convenient parameterizations can be employed according to the specific algorithm applied for inverse analysis. Thus, the function $Q(z)$ defined by Eq 22 is such that $Q(z) \in Q_g$, as well as the function defined by

$$Q(z) = Q_1 \cdot \exp[-\alpha_1 z - \alpha_2 z^2] + Q_2 \cdot \max\left[1 - \frac{2}{1 + \exp[-\beta(z - z_c)]}, 0\right] \quad (\text{Eq 26})$$

Similarly, a discrete representation that should be convenient for numerical procedures applied to inverse analysis is defined by

$$Q(z) = \sum_{k=1}^{N_k} q(z_k) \delta(z - z_k), \quad (\text{Eq 27})$$

such that $Q(z) \in Q_g$, $\delta(z)$ is the Dirac delta function, and $\{q(z_k), z_k\}$, $k = 1, \dots, N_k$, represent adjustable parameters.

6. Basis Functions for Representation of Beam Source Function

A consistent parameterization of the spatial characteristics of beam sources, e.g., laser and electron, above the surface of the workpiece is significant for process parameterization and control. With respect to penetration depth, in this case within a gas medium, the general functional trend of a beam

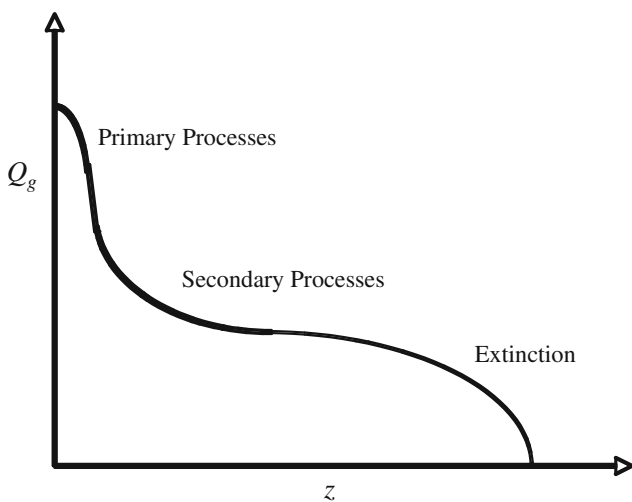


Fig. 4 Generalized function representation of volumetric energy distribution as a function of penetration depth that is characteristic of energy deposition processes

distribution is again that of the generalized function Q_g . Accordingly, a general representation of a beam distribution is given by

$$Q_B(r, \theta) = \sum_{i=1}^{N_i} w_i Q_g(\alpha_{1i} \alpha_{2i} r) + \sum_{j=1}^{N_j} w_j \exp[Q_g(\alpha_{1j} \alpha_{2j} r)] \quad (\text{Eq 28})$$

where the second term provides a formal representation of large changes in beam intensity with increases depth that are multiscale in character. This follows because if $Q(z) \in Q_g$, then $\exp[Q(z)] \in Q_g$. A physically consistent general representation of the coefficients α_{1k} follows from the fact that beam attenuation within a gas medium can be associated with scattering processes, and thus

$$\alpha_{1k}(\theta) = \sum_{n=0}^{N_n} C_{kn} \cos^n \theta. \quad (\text{Eq 29})$$

A physically consistent general representation of the coefficients α_{2k} is that of a constant parameter. The physical interpretation of this parameter follows from the relation

$$\alpha_{2k} = \mu(E)C = c_o E^{-\gamma} C \quad (\text{Eq 30})$$

where $\mu(E)$ is the scattering cross section as a function of energy and C is the concentration of scatterers. It follows that increases and decreases in the value of the parameter α_{2k} correspond to decreases and increases in beam energy, respectively, and increases and decreases in the density of the ambient medium, respectively. Finally, for many types of beam or spray energy sources there can be forward weighting of the spatial distribution due to source geometry. This global trend can be represented by multiplication of Eq 28 a spatial filtering function. Accordingly, a general basis function for beam representation is

$$I(r, \theta) = Q_B(r, \theta) \cdot \exp\left[-\frac{\theta^2}{2\langle\theta\rangle^2}\right] \cos^n \theta \quad (\text{Eq 31})$$

where $\langle\theta\rangle$ and n are adjustable parameters and a consistent parametric representation of the beam intensity distribution is given by

$$I(r, \theta, \cdot) = \sum_{k=1}^{N_k} I_k(r_k, \theta - \theta_k, \cdot), \quad (\text{Eq 32})$$

where constraint conditions are imposed on the I -field spanning the spatial domain above the workpiece by minimizing the value of the objective function defined by

$$Z_B = \sum_{n=1}^N w_n (I(r_n, \theta_n, \cdot) - I_n^c)^2 \quad (\text{Eq 33})$$

where I_n^c is the target intensity for position (r_n, θ_n) . A detailed example of the procedure defined by Eq 32 and 33 is given in Ref 60 for electron beams propagating in air.

7. An Illustrative Example

The analysis presented in this section is typical of many inverse analyses that have been presented previously and

provides a point of reference for describing a general procedure for constructing a multidimensional field representation of energy deposition processes. As discussed previously, with respect to inverse modeling, detailed knowledge of the thermal diffusivity and of the characteristics of the energy deposition process is not necessary for calculation of the temperature field associated with the process considered. This analysis considers a Gas Metal Arc Weld (GMAW) on a 304L stainless steel plate that was instrumented with a thermocouple in order to measure data concerning the temperature profile near the weld (see Fig. 5a). The steel plate was prepared with a V groove as shown graphically in Fig. 5(b). With respect to the inverse analysis procedure considered here, this groove is associated with the volumetric source function $C(\hat{x}_k)$. A type K thermocouple was spot welded on top of the plate next to the weld joint. The temperature history measured by this thermocouple is shown in Fig. 4(c). A Miller Maxtron 450 GMAW welding system with a Miller 60M controller was used to feed 0.035 in 308 stainless steel weld wire through a Miller torch. The distance of the torch contact tip to the bottom of the weld groove was 0.5 in. and the wire feed rate was 390 ipm during the entire weld. Figures 6 and 7 show two-dimensional slices of three-dimensional temperature fields calculated according to the inverse analysis procedure described in the previous sections, at the midplane and top surface of workpiece, respectively. These calculations adopt as adjustable quantities the diffusivity κ and the volumetric source function $C(\hat{x}_k)$ so that the calculated cross sections of the solidification boundaries and temperature field satisfy the specified constraint conditions at the location $\hat{x}_S \in S_0$ of the thermocouple (see Fig. 5c) and positions $(v_c, z_c) \in S_i$ on the transverse cross section of the solidification boundary (see Table 1).

The temperature field shown in Fig. 6(a) and 7(a) satisfy both of the above constraint conditions, i.e., $\hat{x}_S \in S_0$ and S_i , (Fig. 5c and Table 1), while that shown in Fig. 6(b) and 7(b) satisfies only the constraint conditions on the solidification boundary, i.e., $\hat{x}_S \in S_i$. It is interesting to note that the value of the diffusivity adopted for calculation of the temperature fields satisfying both constraints is that of the average diffusivity measured experimentally for 304 stainless steel. A key point demonstrated by this prototype analysis is that information concerning detailed aspects of the heat deposition process is not necessary and that distributed constraint conditions on the temperature field obtained from experiment are sufficient for a complete specification of the temperature field within the workpiece.

8. Construction of a Multidimensional Field Representation

8.1 For Heat Deposition Processes

The set of basis functions presented above provide a general parametric representation for inverse analysis of heat deposition processes. Given these basis functions, the temperature field associated with any given heat deposition process is completely specified by a given set of inner and outer bounding surfaces S_i and S_0 , respectively, the temperature distributions over these surfaces, the diffusivity κ , speed of deposition V , and the lengths of the spatial dimensions D_i of the workpiece. It follows that one can define a multidimensional temperature field

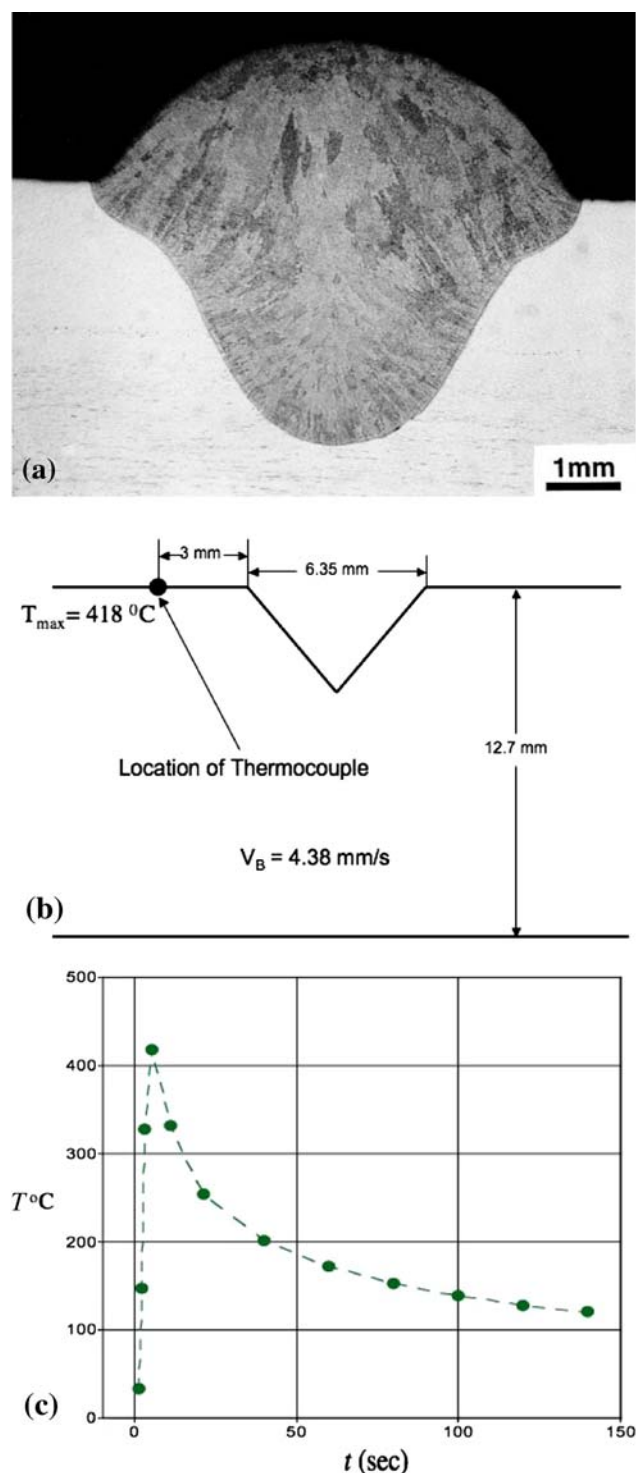


Fig. 5 (a) Transverse cross section of a GMA weld on a 304L stainless steel plate representing inner boundary surface S_i . (b) Graphic representation of steel plate with V groove, showing relative location of thermocouple and representing outer boundary surface S_0 . (c) Temperature history measured by thermocouple located at top surface of workpiece and adjacent to weld bead

$T(\hat{x}, \kappa, V, D_i, T_s(\hat{x}_S), \hat{x}_S \in S_i, S_0)$. At this stage it is significant to note that the multidimensional temperature field $T(\hat{x}, \kappa, V, D_i, T_s(\hat{x}_S), \hat{x}_S \in S_i, S_0)$ represents a parametric representation of heat deposition processes to the extent that any of

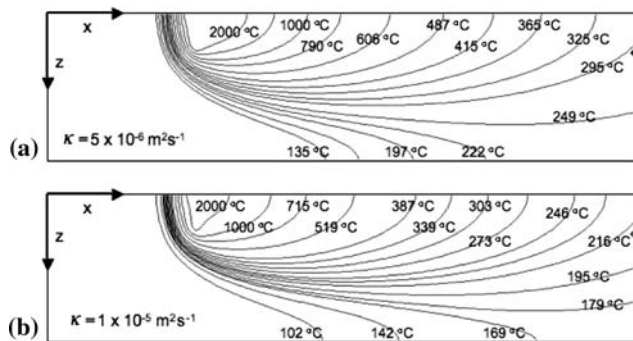


Fig. 6 Longitudinal slices of three-dimensional temperature fields at midplane of model GMA welds, i.e., along xz -plane at $y = 0$, corresponding to different thermal diffusivities. (a) $\kappa = 5 \times 10^{-6} \text{ m}^2 \text{ s}^{-1}$, (b) $\kappa = 1 \times 10^{-5} \text{ m}^2 \text{ s}^{-1}$

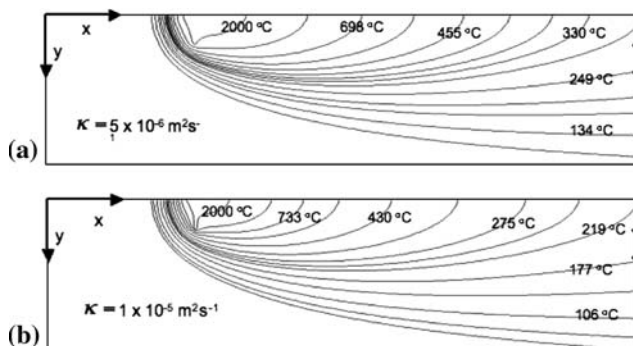


Fig. 7 Longitudinal slices of three-dimensional temperature fields at top surface workpiece for model GMA welds, i.e., along xy -plane at $z = 0$, corresponding to different thermal diffusivities. (a) $\kappa = 5 \times 10^{-6} \text{ m}^2 \text{ s}^{-1}$, (b) $\kappa = 1 \times 10^{-5} \text{ m}^2 \text{ s}^{-1}$

Table 1 Temperature field constraint conditions at the thermocouple location and positions (y_c, z_c) on the transverse cross section of the solidification boundary

Solidification boundary
(y_c mm, z_c mm)

(3.25, 0.0)
(2.5, 0.75)
(1.9, 1.7)
(1.5, 2.5)
(1.0, 3.0)
(0.0, 3.5)

the different possible types of boundary surfaces S_i and S_0 , associated with these processes can be represented using a convenient parametric representation. This is certainly the case since the volumetric source function $C(\hat{x}_k)$ assumes the role of a boundary surface generator, and therefore provides a framework for parametrization of S_i and S_0 using the basis functions given above.

A general procedure for construction of a multidimensional field representation of heat deposition processes can now be described using the illustrative example given above and results of inverse analyses presented previously. The basis of this procedure is that for energy deposition processes for a given

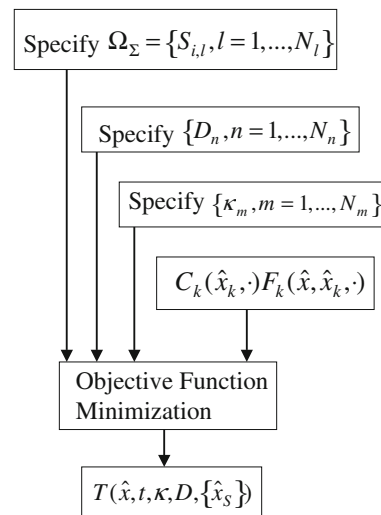


Fig. 8 General procedure for construction of multidimensional temperature field representation of energy deposition processes using a set of reasonable estimates of internal boundary surfaces

class of materials, e.g., metals, the range of different possible shapes of inner boundary surfaces S_i is denumerably finite and that diffusivities and workpiece dimensions are bounded within a relatively small range of values. This procedure may be undertaken by means of two approaches. One approach, which is evolutionary, is based on a systematic accumulation of results of inverse analyses applied to various types of experimental measurements and numerical simulations, while the other approach is based on an initial construction of a finite set of reasonable estimates of internal boundary surfaces. These two approaches to a general procedure for construction of a multidimensional temperature field representation can be described with reference to Fig. 7 and 8. Figure 7 shows the general procedure for calculation of temperature fields for energy deposition processes using inverse analysis. Referring to this figure, it is to be noted that the results of various inverse analyses, e.g., Ref 20-30, involving different types of deposition processes can be stored. In addition, as in the illustrative example given above, for a given inverse analysis where S_i has been specified, one can vary κ and D_i over their entire range of possible values and then store the associated temperature fields. A natural consequence of the finite range of shapes of S_i and of values of κ and D_i is that the stored temperature fields can evolve into a discrete multidimensional temperature field that is sufficiently dense for interpolation between field values. Again referring to Fig. 7, it can be noted that a discrete multidimensional temperature field, having been constructed and sufficiently dense, can be used for objective function minimization as an alternative to parametric representation using basis functions. Referring to Fig. 8, it is to be noted that the finite range of shapes of S_i and of values of κ and D_i provides a foundation for a relatively direct approach to the construction of a multidimensional temperature field. This approach requires, however, the construction of a finite set of reasonable estimates of internal boundary surfaces S_i , which are physically realistic for a sufficient range of energy inputs. Finally, referring to Fig. 9, it is seen that the procedure for construction of multidimensional temperature field can be extended to include dependence on material and beam properties. It is significant to note that the temperature field having been

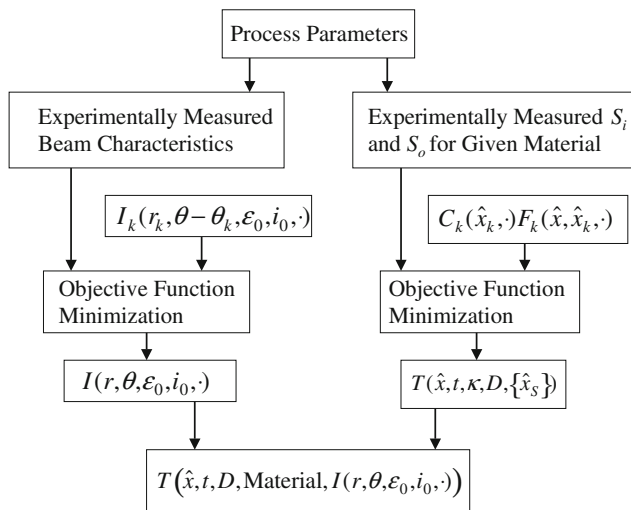


Fig. 9 General procedure for construction of multidimensional temperature field that includes dependence on material and beam properties

constructed is independent of process parameters. This implies that the multidimensional temperature field can be extended to be a function of the physical characteristics of the beam energy source.

9. Conclusion

The objective of this report was to construct a general set of basis functions for parametric representation of all types of energy deposition processes and to describe a general procedure for using these basis functions with available experimental and numerical data to construct a multidimensional temperature field representation of a large class of energy deposition processes. The specific algorithmic aspects of constructing this multidimensional field are for further investigation. This report represents an initial attempt to make quantitative a highly qualitative experience having occurred over the course of inverse analyses applied to various types of energy deposition processes. This experience is associated with the fact that in many cases where inverse analysis, following the procedure defined here, was applied to a given welding process, for a given set of process parameters and alloy, the temperature field having been calculated was very similar to the one having been calculated previously for a significantly different welding process, set of process parameters and alloy. Accordingly, this experience strongly suggests the existence of a multidimensional temperature field $T(\hat{x}, \kappa, V, D_i, T_s(\hat{x}_s), \hat{x}_s \in S_i, S_0)$ for representation of energy deposition processes in general, especially in the case of restricted geometries such as those associated with plate structures. In that the inverse analysis of electron and laser beam spatial distributions associated with energy deposition follow the same formal procedure as that applied to volumetric energy deposition within a material, the multidimensional temperature field should be extendable to being a function of physical characteristics of beam energy sources. Again, the specific algorithmic aspects of this extension require further investigation.

References

1. D.N. Ghosh Roy, *Methods of Inverse Problems in Physics*, CRC Press, Boca Raton, 1991
2. K.A. Woodbury, ed., *Inverse Engineering Handbook*, CRC Press, New York, 2003
3. A. Tarantola, *Inverse Problem Theory and Methods for Model Parameter Estimation*, SIAM, Philadelphia, PA, 2005
4. C.R. Vogel, *Computational Methods for Inverse Problems*, SIAM, Philadelphia, PA, 2002
5. P.C. Sabatier, ed., *Inverse Problems: An Interdisciplinary Study*, Academic Press, London, 1987
6. C.W. Groetsch, *Inverse Problems in the Mathematical Sciences*, Vieweg, Braunschweig, Wiesbaden, 1993
7. A. Kirsch, *An Introduction to the Mathematical Theory of Inverse Problems*, Springer-Verlag, New York, 1996
8. A.G. Ramm, *Inverse Problems, Mathematical and Analytical Techniques with Applications to Engineering*, Springer Science, New York, 2005, p 9–10
9. I.J.D. Craig and J.C. Brown, *Inverse Problems in Astronomy, A Guide to Inversion Strategies for Remotely Sensed Data*, Adam Hilger Ltd., Bristol, 1986
10. M.N. Ozisik and H.R.B. Orlande, *Inverse Heat Transfer, Fundamentals and Applications*, Taylor and Francis, New York, 2000
11. K. Kurpisz and A.J. Nowak, *Inverse Thermal Problems*, Computational Mechanics Publications, Boston, 1995
12. O.M. Alifanov, *Inverse Heat Transfer Problems*, Springer, Berlin, 1994
13. J.V. Beck, B. Blackwell, and C.R. St. Clair, *Inverse Heat Conduction: Ill-Posed Problems*, Wiley Interscience, New York, 1985
14. J.V. Beck, *Inverse Problems in Heat Transfer with Application to Solidification and Welding, Modeling of Casting, Welding and Advanced Solidification Processes V*, M. Rappaz, M.R. Ozgu, and K.W. Mahin, Eds., The Minerals, Metals and Materials Society, 1991, p 427–437
15. J.V. Beck, *Inverse Problems in Heat Transfer, Mathematics of Heat Transfer*, G.E. Tupholme and A.S. Wood, Eds., Clarendon Press, 1998, p 13–24
16. N. Zabarar, *Inverse Modeling of Solidification and Welding Processes, Modeling of Casting, Welding and Advanced Solidification Processes V*, M. Rappaz, M.R. Ozgu, and K.W. Mahin, Eds., The Minerals, Metals and Materials Society, 1991, p 523–530
17. G.S. Dulikravich and T.J. Martin, *Inverse Shape and Boundary Condition Problems and Optimization, Heat Conduction: Advances in Numerical Heat Transfer*, Chap. 10, Vol 1, W.J. Minkowycz and E.M. Sparrow, Eds., Taylor & Francis, 1996, p 381–426
18. T.J. Martin and G.S. Dulikravich, *Inverse Determination of Boundary Conditions in Steady Heat Conduction with Heat Generation, ASME J. Heat Transf.*, 1996, **118**, p 546–554
19. J. Xie and J. Zou, *Numerical Reconstruction of Heat Fluxes, SIAM J. Numer. Anal.*, 2005, **43**(4), p 1504–1535
20. S.G. Lambrakos and S.G. Michopoulos, *Algorithms for Inverse Analysis of Heat Deposition Processes, Mathematical Modelling of Weld Phenomena*, Vol 8, 847 (Graz, Austria), Verlag der Technischen Universite, 2007
21. S.G. Lambrakos and J.G. Michopoulos, *Computational Parameterization Simplicity and Filtering of Data-Driven Inverse Analysis for Heat Deposition Processes, Proceedings of IDETC/CIE 2006, ASME 2006 International Design Engineering Technical Conferences & Computers and Information in Engineering Conference*, Sept 10–13 (Philadelphia, PA), 2006
22. S.G. Lambrakos and J.O. Milewski, *Analysis of Welding and Heat Deposition Processes Using an Inverse-Problem Approach, Mathematical Modelling of Weld Phenomena*, Vol 7, 1025 (Graz, Austria), Verlag der Technischen Universite, 2005, p 1025–1055
23. P.G. Moore, H.N. Jones III, and S.G. Lambrakos, *An inverse Heat Transfer Model of Thermal Degradation within Multifunctional Tensioned Cable Structures, J. Mater. Eng. Perform.*, 2005, **14**(1)
24. S.G. Lambrakos and J.O. Milewski, *Analysis of Processes involving Heat Deposition Using Constrained Optimization, Sci. Technol. Weld. Join.*, 2002, **7**(3), p 137
25. S.G. Lambrakos and D.W. Moon, *Analysis of Welds Using Geometric Constraints, Computer-Aided Design, Engineering, and Manufacturing, Systems Techniques and Applications*, C. Leondes, Ed. (New York), CRC Press, 2001

26. S.G. Lambrakos, E.A. Metzbower, J.O. Milewski, G. Lewis, R. Dixon, and D. Korzekwa, Simulation of Deep Penetration Welding Processes Using Geometric Constraints Based on Experimental Information, *J. Mater. Eng. Perform.*, 1994, **3**(5), p 639
27. K.P. Cooper and S.G. Lambrakos, Fabrication of Net-Shaped Metallic Parts by Overlapping Reinforcement Weld Beads, *Proceedings of the Seventh International Conference on Trends in Welding Research*, May 16-20 (Materials Park, OH, Pine Mountain, GA), ASM International, 2005, p 647
28. E.A. Metzbower, D.W. Moon, C.R. Feng, S.G. Lambrakos, and R.J. Wong, Modelling of HSLA-65 GMAW Welds, *Mathematical Modelling of Weld Phenomena*, Vol 7 (Graz, Austria), Verlag der Technischen Universite, 2005, p 327-339
29. S.G. Lambrakos, R.W. Fonda, J.O. Milewski, and J.E. Mitchell, Analysis of Friction Stir Welds Using Thermocouple Measurements, *Sci. Technol. Weld. Join.*, 2003, **8**, p 345
30. R.W. Fonda and S.G. Lambrakos, Analysis of Friction Stir Welds Using an Inverse Problem Approach, *Sci. Technol. Weld. Join.*, 2002, **7**(3), p 177
31. J. Hadamard, 'Sur les problèmes aux dérivées partielles et leur signification physique', Princeton University Bulletin, 49-52, 1902
32. *Proceedings International Conferences on Trends in Welding Research*, Vol 1-7 (Materials Park, OH), ASM International
33. *Mathematical Modelling of Weld Phenomena*, Vol 1-8 (Graz, Austria), Verlag der Technischen Universite
34. J.A. Goldak and M. Akhlaghi, *Computational Welding Mechanics*, Springer Science+Business Media, Inc., 2005
35. J. Goldak, A. Chakravarti, and M. Bibby, A New Finite Element Model for Welding Heat Source, *Metall. Trans. B*, 1984, **15**, p 299-305
36. J. Goldak, M. Bibby, J. Moore, R. House, and B. Patel, Computer Modeling of Heat Flow in Welds, *Metall. Trans. B*, 1986, **17**, p 587-600
37. R.N. Bracewell, *The Fourier Transform and Its Applications*, 2nd ed., McGraw-Hill Book Company, New York, 1986, p 345-355
38. V.A. Karkhin, V.V. Plochikhine, A.S. Ilyin, and H.W. Bergmann, Inverse Modelling of Fusion Welding Process, in *Mathematical Modelling of Weld Phenomena 6*, ed., H. Cerjak, Ed., Maney Publishing, London, 2002, p 1017-1042
39. V.A. Karkhin, V.V. Plochikhine, and H.W. Bergmann, Solution of Inverse Heat Conduction Problem for Determining Heat Input, Weld Shape, and Grain Structure During Laser Welding, *Sci. Technol. Weld. Join.*, 2002, **7**(4), p 224-231
40. V.A. Karkhin, P.N. Homich, and V.G. Michailov, Models for Volume Heat Sources and Functional-Analytic Technique for Calculating the Temperature Fields in Butt Welding, *Mathematical Modelling of Weld Phenomena*, Vol 8 (Graz, Austria), Verlag der Technischen Universite, 2007, p 847
41. V.A. Karkhin, V.G. Michailov, and V.D. Akatsevich, Modelling the Thermal Behaviour of Weld and Heat-Affected Zone During Pulsed Power Welding, in *Mathematical Modelling of Weld Phenomena 4*, ed., H. Cerjak, Ed., The University Press, Cambridge, 1998, p 411-426
42. S. Kou, *Welding Metallurgy*, 2nd ed., Wiley-Interscience, Hoboken, NJ, 2002
43. E.A. Metzbower, Laser Beam Welding: Thermal Profiles and HAZ Hardness, *Weld. J.*, 1990, **69**(7), p 272
44. I. Tosello, F.X. Tissot, and M. Barras, Modelling of Weld Behaviour for the Control of the GTA Process by Computer Aided Welding, in *Mathematical Modelling of Weld Phenomena 4*, ed., H. Cerjak and H.K.D.H. Bhadeshia, Eds., IOM Communications Ltd., London, 1998, p 80-103
45. R.C. Reed and H.K.D.H. Bhadeshia, A Simple Model For Multipass Welds, *Acta Metall. Mater.*, 1994, **42**(11), p 3663-3678
46. M. Maalekian, E. Kozeschnik, H.P. Brantner, and H. Cerjak, Inverse Modelling of Heat Generation in Friction Welding, *Mathematical Modelling of Weld Phenomena*, Vol 8 (Graz, Austria), Verlag der Technischen Universite, 2007, p 881-890
47. N.N. Rykalin, *Thermal Fundamentals of Welding*, USSR Academy of Sciences, Moscow-Leningrad, 1947
48. N.N. Rykalin, *Calculation of Heat Flow in Welding*, Z. Paley and C.M. Adams, Trans., 1951
49. N.N. Rykalin, *Berchnung der Wdrmevorgange beim Schweissen*, VEB, Verlag Technik, Berlin, 1957
50. N.N. Rykalin, Energy Sources for Welding, *Weld. World*, 1974, **12**(9/10), p 227-248
51. P.N. Sabapathy, M.A. Wahab, and M.J. Painter, Numerical Methods to Predict Failure During the In-Service Welding of Gas Pipelines, *J. Strain Anal.*, 2001, **36**(6), p 611-619
52. E. Ranatowski and A. Pocwiardowski, An Analytical-Numerical Evaluation of the Thermal Cycle in the HAZ During Welding, in *Mathematical Modelling of Weld Phenomena 4*, ed., H. Cerjak and H.K.D.H. Bhadeshia, Eds., IOM Communications Ltd., London, 1998, p 379-395
53. E. Ranatowski and A. Pocwiardowski, An Analytical-Numerical Estimation of the Thermal Cycle During Welding with Various Heat Source Models Application, in *Mathematical Modelling of Weld Phenomena 5*, ed., H. Cerjak and H.K.D.H. Bhadeshia, Eds., IOM Communications Ltd., London, 1998, p 723-742
54. E. Ranatowski and A. Pocwiardowski, An Analytical-Numerical Assessment of the Thermal Cycle in HAZ with Three Dimensional Heat Source Models and Pulsed Power Welding, in *Mathematical Modelling of Weld Phenomena 7*, ed., H. Cerjak, H.K.D.H. Bhadeshia and E. Kozeschnik, Eds., Verlag der Technischen Universite, Graz, Austria, 2001, p 1111-1128
55. D. Rosenthal, The Theory of Moving Sources of Heat and Its Application to Metal Treatments, *Trans. ASME*, 1946, **68**, p 849-866
56. D. Rosenthal, Mathematical Theory of Heat Conduction During Welding and Cutting, *Weld. J.*, 1941, **20**(5), p 220-234
57. D. Rosenthal, Etude theoretic du regime thermique pendant la soudure a l'arc, Zieme Congress National des Sciences, Brussels, 1935, p 1277-1292
58. O. Grong, *Metallurgical Modelling of Welding*, Chap. 2, 2nd ed., Materials Modelling Series, H.K.D.H. Bhadeshia, Ed., The Institute of Materials, UK, 1997, p 1-115
59. H.S. Carslaw and J.C. Jaeger, *Conduction of Heat in Solids*, 2nd ed., Clarendon Press, Oxford, 1959, p 374
60. R.F. Fernsler, S.P. Slinker, and S.G. Lambrakos, A Numerical Model and Scaling Relationship for Energetic Electron Beams in Air, *J. Appl. Phys.*, 2008, **104**(6), p 063312